

Liver-specific Deficiency of Serine Palmitoyltransferase Subunit 2 Decreases Plasma Sphingomyelin and Increases Apolipoprotein E Levels*

Received for publication, July 7, 2009 Published, JBC Papers in Press, August 1, 2009, DOI 10.1074/jbc.M109.042028

Zhiqiang Li[‡], Yan Li[‡], Mahua Chakraborty[‡], Yifan Fan[‡], Hai H. Bui[§], David A. Peake[§], Ming-Shang Kuo[§], Xiao Xiao[¶], Guoqing Cao[§], and Xian-Cheng Jiang^{‡,1}

From the [‡]State University of New York Downstate Medical Center, Brooklyn, New York 11203, [§]Lilly Research Laboratories, Eli Lilly and Company, Indianapolis, Indiana 46285, and the [¶]Division of Molecular Pharmaceutics, University of North Carolina Eshelman School of Pharmacy, Chapel Hill, North Carolina 27599

Sphingomyelin (SM) is one of the major lipid components of plasma lipoproteins. Serine palmitoyltransferase (SPT) is the key enzyme in SM biosynthesis. Mice totally lacking in SPT are embryonic lethal. The liver is the major site for plasma lipoprotein biosynthesis, secretion, and degradation, and in this study we utilized a liver-specific knock-out approach for evaluating liver SPT activity and also its role in plasma SM and lipoprotein metabolism. We found that a deficiency of liver-specific *Sptlc2* (a subunit of SPT) decreased liver SPT protein mass and activity by 95 and 92%, respectively, but had no effect on other tissues. Liver *Sptlc2* deficiency decreased plasma SM levels (in both high density lipoprotein and non-high density lipoprotein fractions) by 36 and 35% ($p < 0.01$), respectively, and increased phosphatidylcholine levels by 19% ($p < 0.05$), thus increasing the phosphatidylcholine/SM ratio by 77% ($p < 0.001$), compared with controls. This deficiency also decreased SM levels in the liver by 38% ($p < 0.01$) and in the hepatocyte plasma membranes (based on a lysenin-mediated cell lysis assay). Liver-specific *Sptlc2* deficiency significantly increased hepatocyte apoE secretion and thus increased plasma apoE levels 3.5-fold ($p < 0.0001$). Furthermore, plasma from *Sptlc2* knock-out mice had a significantly stronger potential for promoting cholesterol efflux from macrophages than from wild-type mice ($p < 0.01$) because of a greater amount of apoE in the circulation. As a result of these findings, we believe that the ability to control liver SPT activity could result in regulation of lipoprotein metabolism and might have an impact on the development of atherosclerosis.

Sphingomyelin (SM),² an amphipathic phospholipid located in the surface monolayer of all classes of plasma lipoproteins

(LDL/very low density lipoprotein, 70–75%; HDL, 25–30%) (1), has significant effects on lipoprotein metabolism.

A number of studies indicate that plasma SM levels influence the metabolism of apoB-containing lipoproteins. It has been reported that SM, but not cholesterol, significantly inhibits triglyceride lipolysis by lipoprotein lipase (2, 3). It has also been found that SM in lipoproteins delays remnant clearance by decreasing the binding of apoE to cell membrane receptors (4).

Plasma SM levels also influence high density lipoprotein (HDL) metabolism. There have been reports that SM affects the structure of discoidal and spherical HDL (5). SM can inhibit lecithin-cholesterol acyltransferase by decreasing its binding to HDL (6). A negative correlation between the SM content of HDL and lecithin-cholesterol acyltransferase activity was observed in studies with proteoliposomes or reconstituted HDL (7). SM-rich recombinant HDL can inhibit scavenger receptor class B type I-mediated cholesterol ester-selective uptake in HepG2 cells (8).

It is known that subendothelial retention and aggregation of atherogenic lipoproteins play an important role in atherogenesis (9). LDL extracted from human atherosclerotic lesions is highly enriched in SM than in plasma LDL (10–13). LDL retained in atherosclerotic lesions is acted on by an arterial wall sphingomyelinase, which promotes aggregation by converting SM to ceramide (10–12). Sphingomyelinase deficiency diminishes lipoprotein retention within early atheromata and prevents lesion progression (14). The ratio of SM to PC is increased 5-fold in very low density lipoprotein from hypercholesterolemic rabbits (15). *ApoE* knock-out (KO) mice are a well known atherogenic model. It has been shown that plasma SM levels in these mice are 4-fold higher than in WT animals (16), and this may contribute to increased atherosclerosis (17, 18). It has also been shown that in humans, higher plasma SM levels and SM/PC ratios are independent risk factors for coronary heart disease (19, 20). All these data suggest that plasma SM plays a critical role in the development of atherosclerosis.

The interaction of SM, cholesterol, and glycosphingolipids drives the formation of plasma membrane rafts (21). These rafts, formed in the Golgi apparatus, are targeted to the plasma membranes, where they are thought to exist as islands within

* This work was supported, in whole or in part, by National Institutes of Health Grants HL-64735 and HL-69817 (to X.-C. J.). This work was also supported by an American Heart Association grant-in-aid (to X.-C. J.).

¹ To whom correspondence should be addressed: State University of New York Downstate Medical Center, 450 Clarkson Ave., Box 5, Brooklyn, NY 11203. Tel.: 718-270-6701; Fax: 718-270-3732; E-mail: XJiang@downstate.edu.

² The abbreviations used are: SM, sphingomyelin; SPT, serine palmitoyltransferase; *Sptlc2*, serine palmitoyl-CoA long chain base 2; KO, gene knockout; apoE, apolipoprotein E; PC, phosphatidylcholine; WT, wild type; HDL, high density lipoprotein; LDL, low density lipoprotein; DMEM, Dulbecco's modified Eagle's medium; FBS, fetal bovine serum; PBS, phosphate-buffered saline; HPLC, high pressure liquid chromatography; AAV, adeno-associated virus; FPLC, fast protein liquid chromatography; MS/MS, tandem mass

spectrometry; LC, liquid chromatography; ESI, electrospray ionization; X-gal, 5-bromo-4-chloro-3-indolyl- β -D-galactopyranoside.

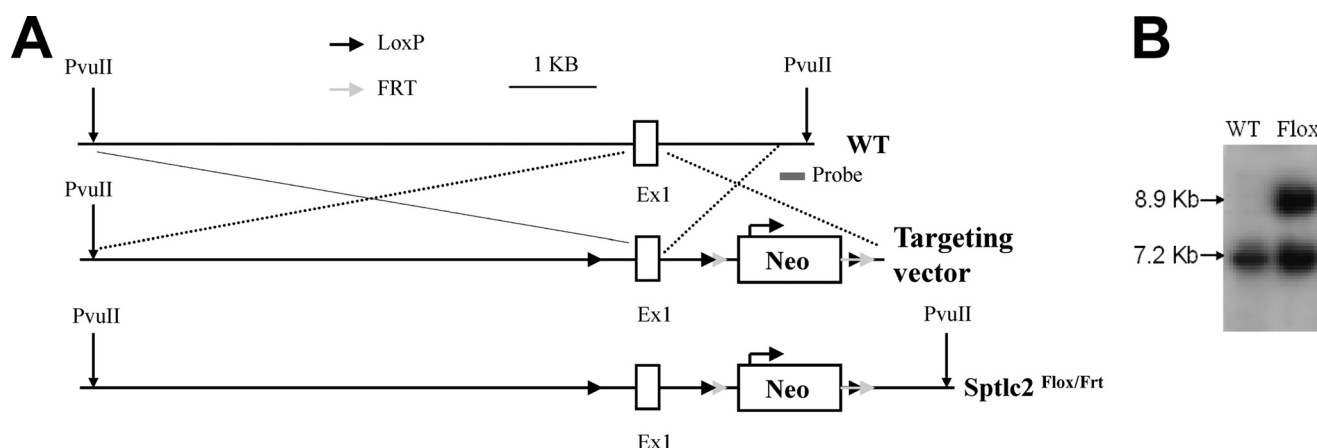


FIGURE 1. *Sptlc2*^{Flox-FRT} mouse preparation. *A*, strategy for *Sptlc2*^{Flox-FRT} mouse preparation. An Loxp site was inserted in the 5'-flanking region of the *Sptlc2* gene. A neomycin-resistant gene (*Neo*) cassette, flanked with a pair of Loxp sites and a pair of FRT sites, was inserted into intron 1, creating the targeting vector. A probe complementary to a 330-bp fragment of the gene 3' to the targeting vector was used, first for successfully detecting targeted embryonic stem cells and subsequently screening for positive mice. *B*, Southern blot of WT and *Sptlc2*^{Flox-FRT} mice. The WT mouse has a 7.2-kb PvuII-digested signal; the heterozygous Flox animal has 7.2- and 8.9-kb signals.

the sea of bulk membrane. Although there is disagreement as to their content, rafts are considered in most reports to include about 3500 lipid molecules and 30 proteins (22). As much as 65% of the total cellular SM is located in these rafts (23). Manipulation of membrane SM levels by sphingomyelinase can alter lipid raft composition, thus modifying cell function. For example, cholesterol efflux from macrophage foam cells, a key step in reverse cholesterol transport, requires trafficking of cholesterol from intracellular sites to the plasma membranes. Sphingomyelinase deficiency decreases cholesterol efflux through promoting cholesterol sequestration by SM (24).

The biochemical synthesis of SM occurs through the actions of serine palmitoyl-CoA transferase (SPT), 3-ketosphinganine reductase, ceramide synthase, dihydroceramide desaturase, and sphingomyelin synthase. Located in the endoplasmic reticulum membranes, SPT is the rate-limiting enzyme in the pathway (25). Mammalian SPT contains two subunits, *Sptlc1* and *Sptlc2*, encoding 53- and 63-kDa proteins, respectively (26, 27). Data from *in vivo* and *in vitro* studies suggest that each subunit is stabilized by forming a dimer (or possibly larger multimer) with the other (28). Another subunit, *Sptlc3*, has been reported (29), and it is important that its functions be further characterized.

Mice totally lacking *Sptlc1* or *Sptlc2* are embryonic lethal (30). Because the liver is the major site for plasma lipoprotein biosynthesis, secretion, and degradation, we utilized a liver-specific knock-out approach for evaluating liver SPT activity and its role in plasma SM and lipoprotein metabolism. We found that *Sptlc2* deficiency in the liver decreases plasma SM and increases apoE levels.

EXPERIMENTAL PROCEDURES

Reagents

Bovine brain L- α -phosphatidylcholine (PC), 12-(*N*-methyl-*N*-(7-nitrobenz-2-oxa-1,3-diazol-4-yl))-C₆-ceramide, and lysenin were purchased from Sigma. [³⁵S]Methionine was from Amersham Biosciences. WST-1 cell proliferation reagent was from Roche Applied Science. The 16:0, 18:0, 20:0, 24:0, and 24:1 ceramides, 17:0 sphingomyelin, and 14:0 phosphatidylcholine

were from Avanti. Labeled 18:0 and 24:0 ceramides were synthesized internally at Eli Lilly and Co. The 15:0 1,3-dipentadecanoin was from Sigma.

Liver-specific *Sptlc2* KO Mouse Preparation

The overall strategy for gene targeting was to delete exon 1 from *Sptlc2*. Because exon 1 contains the translation codon ATG, its deletion would be expected to create a null *Sptlc2* mouse model.

Sptlc2^{Flox-FRT} Mouse Preparation

Through homologous recombination in mouse embryonic stem cells (with a C57BL/6 background), we inserted an Loxp site in the 5'-flanking region of the *Sptlc2* gene and then a neomycin resistance gene (*Neo*) cassette, flanking with one pair of Loxp and one pair of FRT (Fig. 1*A*), into intron 1. Five positive clones were identified out of 210 screened (Fig. 1*B*), and were injected into blastocysts. Chimeric males were mated with WT females. Ten heterozygous *Sptlc2*^{Flox-FRT} mice were obtained with a C57BL/6 background.

Sptlc2 ^{Δ Neo} Mouse Preparation

We deleted the *Neo* cassette by crossing heterozygous *Sptlc2*^{Flox-FRT} mice with Flp transgenic ones (Fig. 2*A*) (31, 32) from The Jackson Laboratory. We obtained 10 mosaic mice with *Sptlc2* ^{Δ Neo} (Fig. 2*B*) and crossed them with WT animals to establish 100% heterozygous *Sptlc2* ^{Δ Neo} animals (Fig. 2*C*).

Sptlc2-flox Mouse Preparation

Heterozygous *Sptlc2* ^{Δ Neo} mice were crossed with each other (Fig. 2*D*).

Liver-specific *Sptlc2*-deficient Mouse Preparation

We injected (intravenously) adeno-associated virus (AAV)-Cre and AAV-LacZ (2×10^{11} particles/animal) into 14 *Sptlc2*-Flox mice (seven each), according to a published report (33). One month later, we sacrificed the animals and carried out our study. During this period, all animals were normal in terms of

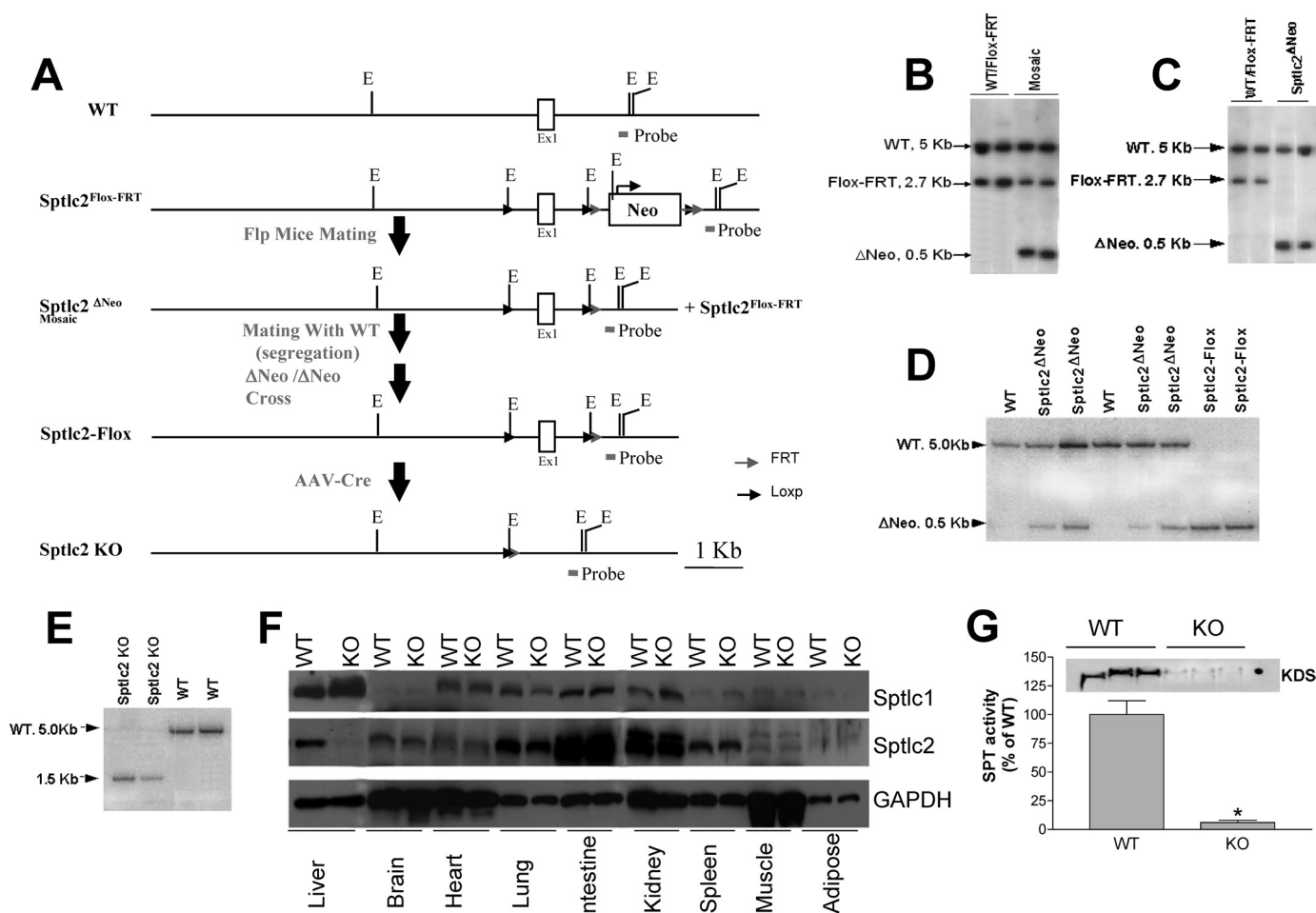


FIGURE 2. Liver-specific *Sptlc2* KO mouse preparation. *A*, strategy. A 250-bp fragment was used as a probe for Southern blot analysis. *B* and *C*, preparation of *Sptlc2*^{ΔNeo} mice. To delete the Neo cassette in the *Sptlc2*^{Flox-FRT} mice, we crossed heterozygous *Sptlc2*^{Flox-FRT} animals with Flp transgenic ones. To facilitate screening for success of the deletion, we designed an internal 250-bp probe for Southern blot analysis. The mosaic (WT + Flox-FRT + ΔNeo) animal has 5.0-, 2.7-, and 0.5-kb signals (*B*); and the heterozygous mouse (WT/Flox-FRT) has 5.0- and 2.7-kb EcoRI digested signals (*C*). *D*, preparation of *Sptlc2*-Flox mice. Heterozygous *Sptlc2*^{ΔNeo} ones were crossed with each other, thus creating *Sptlc2*-Flox (homozygous for *Sptlc2*^{ΔNeo}) animals. *E*, *Sptlc2*-Flox mice were injected with AAV-Cre and AAV-LacZ, respectively. One month later, total genomic DNA was extracted from the liver, and Southern blot was performed to confirm deletion of the *Sptlc2* gene. *F*, Western blot analysis of Sptlc1 and Sptlc2 in different tissues to indicate liver specificity. Glyceraldehyde-3-phosphate dehydrogenase (GAPDH) was a loading control. *G*, liver SPT activity measurement. These are results from three different animals in both WT and *Sptlc2* KO groups. *E*, EcoRI.

body weight gain, daily activity, eating, and drinking. We also carried out lipid analysis 2 months after AAV injection.

Western Blot for Mouse Liver *Sptlc1* and *Sptlc2*

SDS-PAGE was performed on 4–15% SDS-polyacrylamide gradient gel, using mouse liver homogenate (200 μg of protein), and the separated proteins were transferred to nitrocellulose membrane. Western blot analysis for Sptlc1 was performed, using polyclonal anti-mouse Sptlc1 antibody (Pharmingen). Analysis for Sptlc2 was done with polyclonal anti-rabbit Sptlc2 antibody generated by Proteintech Group, Inc., according to the mouse Sptlc2 peptide sequence, ⁵³⁶KYSRHRLVPLDRPFDETTYEETED⁵⁶⁰. Horseradish peroxidase-conjugated rabbit polyclonal antibody to mouse IgG (Novus Biologicals) was used as a secondary antibody for Sptlc1, and horseradish peroxidase-conjugated goat polyclonal antibody to rabbit IgG (Novus Biologicals) was used for Sptlc2. The SuperSignal West detection kit (Pierce) was used for detection. Glyceraldehyde-3-phosphate dehydrogenase was used as a loading control. The maximum intensity of each band was measured by Image-Pro Plus version 4.5 software (Media Cybernetics Inc.) and used for analysis.

Tissue SPT Activity Assay

Mouse liver (0.2 g) was homogenized in 0.5 ml of 50 mM Tris-HCl (pH 7.4), 5 mM EDTA, and 250 mM sucrose. SPT activity in the homogenates was measured with [¹⁴C]serine and palmitoyl-CoA as substrates, as described previously (30).

Lipid and Lipoprotein Measurements

Fasting plasma was collected for FPLC separation and lipid measurement. Total cholesterol, phospholipids, and triglyceride in plasma and lipoproteins were assayed by enzymatic methods (Wako Pure Chemical Industries Ltd., Osaka, Japan). Plasma SM was measured as described previously (34).

Apolipoprotein Measurement

Plasma apoE, apoB, and apoA-I levels were determined as described previously (35). Briefly, 0.2 μl of plasma were separated by 4–15% SDS-gel electrophoresis and immunoblotted with polyclonal antibodies against apoE (Abcam), apoB (United States Biological), and apoA-I (Abcam).

Lipid Analysis

LC/ESI/MS/MS analysis of sphingolipids was performed, using a TSQ Quantum Ultra-triple quadrupole mass spectrometer (Thermo Fisher, San Jose, CA) equipped with an ESI probe and interfaced with an Agilent 1100 HPLC (Agilent Technologies, Wilmington, DE). Lipid extracts were separated with an XBridge C8 (Waters). Mobile phase A was methanol/water/formic acid (80:20:0.4% by v/v); mobile phase B was methanol/acetonitrile (50:50% by v/v). Mass spectrometric analyses were performed on line using electrospray ionization-tandem mass spectrometry in the positive multiple reaction monitoring mode. Samples were extracted using the one-phase extraction method (methanol/chloroform) with internal standards. Ceramides, sphingosines, sphingosine 1-phosphate, and dihydrosphingosine 1-phosphate levels were quantified by the ratio of analyte and internal standard and calibration curves obtained by serial dilution of a mixture of sphingolipids.

Phosphatidylcholine and sphingomyelin levels were measured by a flow injection ESI-MS/MS method, adapted from the work of Liebisch *et al.* (36), suitable for rapid monitoring of PC and SM present at micromoles/liter to millimoles/liter levels in plasma, tissue, or cell extracts. The flow injection MS/MS system consisted of a Quattro Ultima triple quadrupole mass spectrometer (Waters) interfaced to an 1100 binary HPLC (Agilent Technologies) and a CTC PAL autosampler (LEAP Technologies, Carrboro, NC) equipped with an active wash station and cycle composer control software.

Protonated molecular ions of PC/SM species were selected by precursor ion scans of m/z 184, the fragment ion containing the positively charged phosphocholine lipid headgroup. The ion intensities across the flow injection profile were summed together, and after isotope correction, the concentrations of each PC/SM species were then calculated relative to PC and SM internal standards, as well as mean response factors obtained from serial dilution of equimolar mixtures containing 12 different PC and 3 SM standards.

Samples (20 μ l of plasma or 20 mg of tissue homogenate in deionized water) were increased by 5 nmol each of 14:0 PC, 21:0 PC, and 17:0 SM internal standards prior to extraction. Sample aliquots were diluted into a total of 0.45 ml of water, containing HCl, and 1.5 ml of 2:1 methanol/chloroform. After mixing thoroughly, 0.5 ml of water and 0.5 ml of chloroform were added. The samples were mixed and centrifuged (4000 rpm, 5 °C) for 15 min. The chloroform layer was removed, evaporated under a stream of warm nitrogen, and reconstituted in 1.00 ml of 75% methanol, 25% chloroform (v/v), 10 mM ammonium acetate, and 10 μ l of the lipid extract was analyzed in duplicate/triplicate.

Lysenin Treatment and Cell Mortality Measurement

Hepatocytes were isolated as described previously (37). Monolayer cells were washed twice with PBS and incubated with 200 ng/ml lysenin, or without it as a control, at 37 °C for 2 h. Cell mortality was measured using WST-1 cell proliferation reagent, according to manufacturer's instructions (Roche Applied Science). Briefly, WST-1 cell proliferation reagent was added to monitor cell mortality. After continuous incubation at

37 °C for 15 min, the solution was transferred to an Eppendorf tube and spun (12,000 rpm) to pellet cell debris. Supernatant was then measured by absorbance at 450 nm, a reading for viable cells.

Cholesterol Efflux

Wild-type macrophages (10^5 cells/well) were grown in DMEM with 10% FBS for 24 h to reach a confluency of about 80%. Cell labeling was done by growing the cells overnight in DMEM with 10% FBS containing 50 μ g/ml acetylated LDL and 1 μ Ci/ml of [3 H]cholesterol. Cells were washed three times with PBS to remove excess label and equilibrated for 2 h with DMEM without FBS. The medium was replaced with DMEM containing 10% plasma from WT and liver-specific *Sptlc2* KO mice. We measured [3 H]cholesterol radioactivity in the medium at 4 and 8 h. We also measured radioactivity inside the cells. The percentage of cholesterol efflux was calculated by dividing the radioactive amounts in the extracellular media by the total of the radioactive amounts in the medium and cell fractions.

Tissue Staining

Hematoxylin and Eosin Staining—All tissues were dissected out and put into 4% paraformaldehyde for fixation overnight. Tissues were paraffin-embedded. All tissues were then sliced (10 μ m thick). Each slice was deparaffinized and stained with hematoxylin and eosin according to the standard procedure.

Oil Red O Staining—Frozen liver sections were stained with Oil Red O working solution for 30 min. The slides were washed with water and then stained with hematoxylin solution for 2 min.

X-gal Staining—Liver sections were stained using an X-gal staining kit (Millipore) according to the manufacturer's protocol. Briefly, frozen liver sections were fixed with cold fixative. The sections were washed and incubated in X-gal working solution at 37 °C in the dark for 24 h. They were then rinsed with PBS and subsequently distilled water. Finally, the sections were mounted directly with aqueous mounting medium.

β -Galactosidase Immunostaining—Frozen liver sections were incubated with anti- β -galactosidase antibody (1:500 dilution) at 4 °C overnight. The sections were washed two times in Tris/saline buffer for 5 min and then incubated with fluorescein isothiocyanate secondary antibody (1:200 dilution) at room temperature in the dark for 1 h. Again in the dark, sections were washed twice with Tris/saline buffer for 5 min. Finally, they were examined under a fluorescent microscope.

Primary Hepatocyte Culture and Immunoprecipitation of ApoE from Culture Medium or Cell Lysate

To investigate the effect of SPT deficiency on apoE secretion, a pulse-chase experiment was used in the study. Mouse primary hepatocytes were isolated and cultured as described previously (37). Cells were pulse-labeled with [35 S]methionine for 30 min and chased for 1 or 2 h. The newly synthesized apoE was immunoprecipitated from cell homogenates and culture medium and analyzed on SDS-PAGE as described previously (37).

Statistical Analysis—Each experiment was conducted at least five times. Data were typically expressed as mean \pm S.D. Data

Liver *Sptlc2* Deficiency and Sphingomyelin Metabolism

between two groups were analyzed by Student's *t* test. Values for *p* of less than 0.05 were considered significant.

RESULTS

Creation of Liver-specific *Sptlc2*-deficient Mice—To determine whether an *Sptlc2* gene deficiency could be specifically generated in the liver, we injected (intravenously) AAV-Cre and AAV-LacZ (2×10^{11} particles/animal) (Fig. 2A) into 14 *Sptlc2*-Flox mice (seven each). One month later, we sacrificed the animals and isolated liver genomic DNA. This was digested with EcoRI, and an internal 250-bp probe was used to analyze Southern blots (Fig. 2A). We thus demonstrated that recombination of the floxed *Sptlc2* alleles (and thereby inactivation of the *Sptlc2* gene) could be achieved in essentially 95% of the hepatocytes after injection of a recombinant AAV carrying the Cre recombinase (Fig. 2E). Because expression of virally transferred exogenous genes, in this case the Cre recombinase, is almost exclusively limited to the liver (33), *Sptlc2* inactivation (95% protein mass) was highly tissue-specific (Fig. 2F). Moreover, *Sptlc2* deficiency caused a 92% decrease in liver SPT activ-

ity (Fig. 2G), compared with controls, although liver *Sptlc1* protein levels were not significantly affected (Fig. 2F).

To investigate whether liver-specific *Sptlc2* KO had any impact on tissue morphology, we stained sections from the liver, heart, small intestine, kidney, and lung with hematoxylin and eosin. As shown in Fig. 3A, neither AAV-Cre nor AAV-LacZ treatment influenced the morphology of any of these tissues. We also stained the liver section with Oil Red O, and we found no difference between AAV-Cre- and AAV-LacZ-treated animals (Fig. 3B). To visualize the efficiency of AAV infection in the liver, we stained frozen section of the liver with X-gal and found that the efficiency of AAV-LacZ infection is roughly 100% (Fig. 3C). We also utilized β -galactosidase immunostaining on liver sections, finding that almost all the hepatocytes were stained after AAV-LacZ infection (Fig. 3D). Thus, we have created liver-specific SPT KO mice.

Plasma Lipid Analysis in Liver-specific *Sptlc2* KO Mice—As indicated in Table 1, plasma lipid analysis showed a significant reduction in SM levels of 36% ($p < 0.001$) for both HDL and non-HDL portions in AAV-Cre-injected mice, compared with AAV-LacZ-injected animals. To our surprise, a small but significant increase of total cholesterol levels in liver-specific *Sptlc2* KO mice was also observed for both HDL and non-HDL portions, an increase of 19% ($p < 0.05$). We determined hydroxymethylglutaryl-CoA reductase mRNA in the liver using real time PCR, finding no significant difference between *Sptlc2* KO animals and controls (data not shown). This indicated that the plasma cholesterol increase in *Sptlc2* KO mice was not because of the enhancement of cholesterol biosynthesis in the liver. There were no significant changes in total phospholipid or triglyceride levels (Table 1).

The distribution of lipids was also measured by FPLC of pooled plasma samples. This confirmed that plasma SM levels were significantly decreased in both HDL and non-HDL fractions from liver *Sptlc2* KO mice, compared with controls (Fig. 4A). HDL and non-HDL cholesterol were increased (Fig. 4B), but there

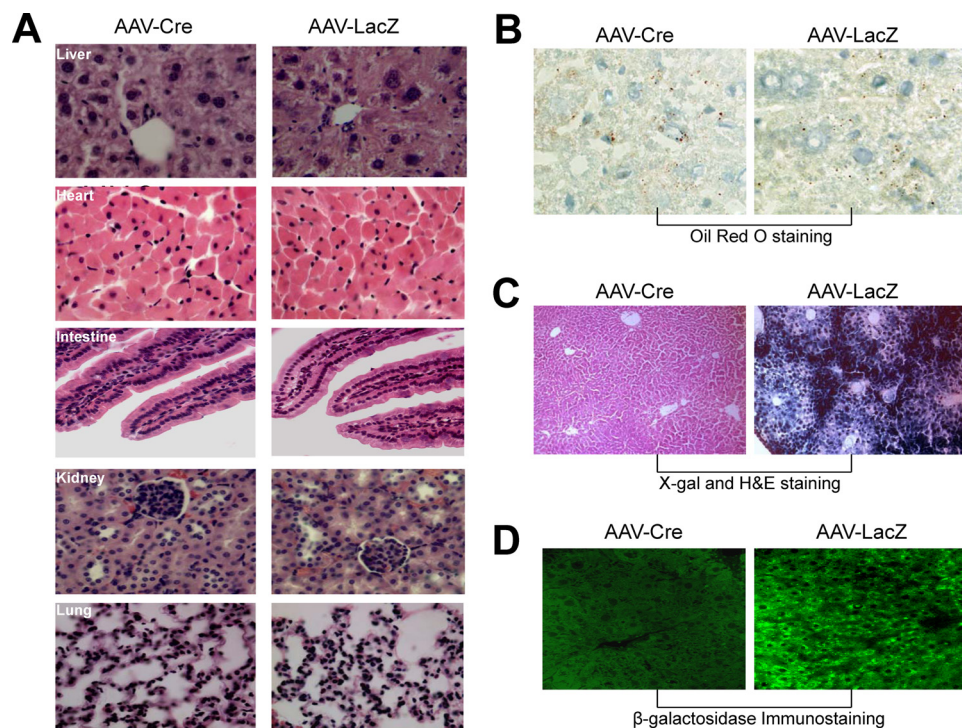


FIGURE 3. Mouse tissue staining. A, liver-specific SPT deficiency changed the morphology of mouse liver, heart, small intestine, kidney, and lung. The tissue was dissected out and put into 4% paraformaldehyde for fixation overnight. The tissue was then sliced (10 μ m thick). Each slice was deparaffinized and stained with hematoxylin and eosin (H&E). The morphology was checked by microscope. B, Oil Red O staining. C, X-gal staining. D, β -galactosidase immunostaining.

TABLE 1

Plasma lipid measurement in liver-specific *Sptlc2* KO and WT mice (enzymatic assay)

Values are as follows: mean \pm S.D.; $n = 5$. The abbreviations used are as follows: SM, sphingomyelin; Chol, cholesterol; PL, phospholipids; TG, triglyceride; HDL-C, HDL cholesterol; HDL-PL, HDL phospholipid.

Mice	SM	HDL-SM	Chol	HDL-C	PL	HDL-PL	TG
WT	25 \pm 5	17 \pm 4	107 \pm 8	86 \pm 7	198 \pm 17	157 \pm 16	47 \pm 8
<i>Sptlc2</i> KO	16 \pm 3 ^a	11 \pm 3 ^b	126 \pm 21 ^b	99 \pm 9 ^b	211 \pm 27	168 \pm 21	50 \pm 7

^a Values are $p < 0.01$.

^b Values are $p < 0.05$.

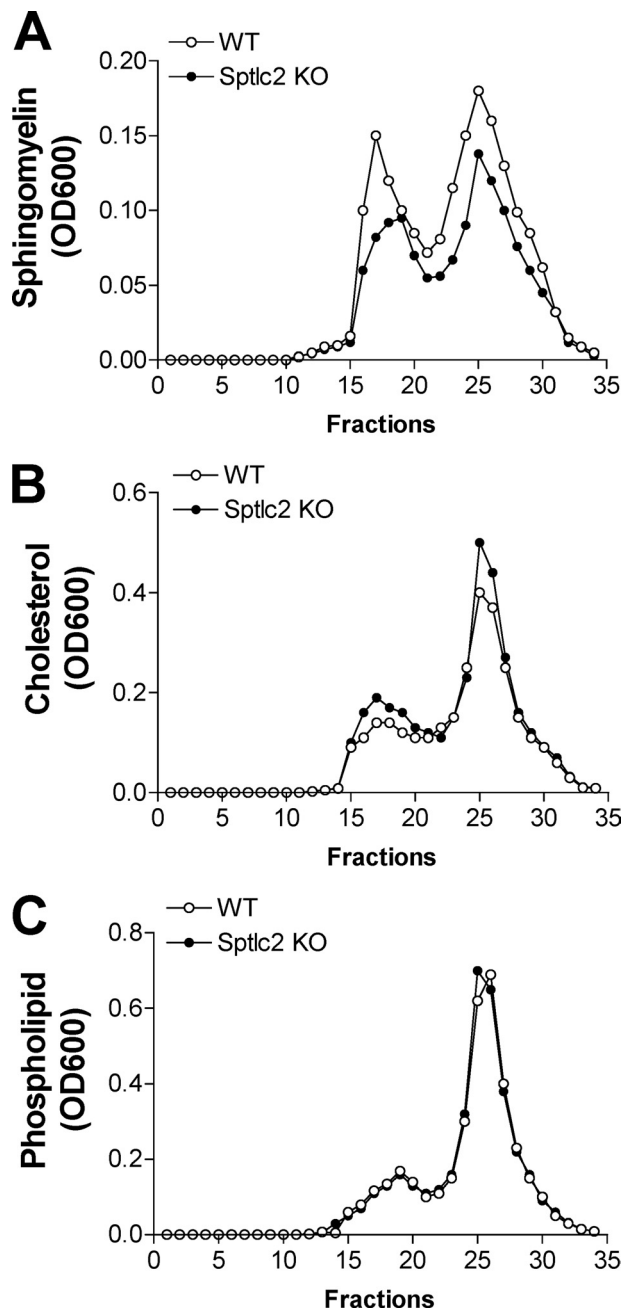


FIGURE 4. **Plasma lipoprotein analysis by FPLC in mice.** A 200- μ l aliquot of pooled plasma (from seven animals) was loaded into a Sepharose 6B column and eluted with 10 mM Tris and 0.15 M NaCl (pH 7.5). An aliquot of each fraction was used for determination of sphingomyelin. *A*, total cholesterol. *B*, total phospholipids. *C*, FPLC fast protein liquid chromatography.

TABLE 2
Plasma lipid measurement in liver-specific *Sptlc2* KO and WT mice (LC/MS/MS)

Values are as follows: mean \pm S.D.; $n = 4-5$. The abbreviations used are as follows: SM, sphingomyelin; Cer, ceramide; Sph, sphingosine; S-1-P, sphingosine 1-phosphate; DHS-1-P, dihydroxyphingosine 1-phosphate.

Mice	SM	PC	PC/SM	Cer	Sph	S-1-P	DHS-1-P
	μ M	μ M		ng/ml	ng/ml	ng/ml	ng/ml
One month							
WT	96 \pm 9	1759 \pm 97	18 \pm 2	1000 \pm 85	23 \pm 2	264 \pm 21	114 \pm 14
<i>Sptlc2</i> KO	61 \pm 5 ^a	2096 \pm 89 ^a	32 \pm 5 ^a	462 \pm 42 ^a	31 \pm 1 ^a	282 \pm 13	99 \pm 13
Two months							
WT	102 \pm 5	1802 \pm 117	21 \pm 3	912 \pm 51	30 \pm 4	302 \pm 44	123 \pm 29
<i>Sptlc2</i> KO	65 \pm 6 ^a	2133 \pm 191 ^a	35 \pm 9 ^a	501 \pm 67 ^a	35 \pm 5	297 \pm 27	135 \pm 39

^a Values are $p < 0.05$.

were no significant changes in total phospholipid levels (Fig. 4C).

To determine whether liver *Sptlc2* deficiency had any impact on plasma sphingolipid levels, MS analysis of ceramide, sphingosine, sphingosine 1-phosphate, and dihydroxyphingosine 1-phosphate was performed. As shown in Table 2, plasma SM levels were again significantly decreased by 36% ($p < 0.01$), whereas plasma phosphatidylcholine (PC) levels were significantly increased by 19% ($p < 0.01$). Thus, the PC/SM ratio was increased by 77% ($p < 0.001$), compared with controls. Moreover, plasma ceramide levels were also significantly decreased by 54% ($p < 0.001$), and sphingosine levels were significantly increased by 35% ($p < 0.01$), whereas there was no change in sphingosine 1-phosphate and dihydroxyphingosine 1-phosphate, compared with controls (Table 2). These results indicated that liver-specific *Sptlc2* deficiency inhibited virtually all liver SPT activity, and dramatically decreased plasma SM levels.

Liver Lipid Analysis in Liver-specific *Sptlc2* KO Mice—As indicated in Table 3, *Sptlc2*-deficient liver contained significantly less SM than controls by 38% ($p < 0.01$). Liver *Sptlc2* deficiency also significantly decreased ceramide and sphingosine in the liver by 39 and 32%, respectively ($p < 0.01$), and increased sphingosine 1-phosphate contents by 38% ($p < 0.01$), compared with controls. There were no significant changes in total cholesterol, phospholipid, or triglyceride levels (data not shown).

We then explored the effect of liver *Sptlc2* deficiency on SM levels in hepatocyte plasma membranes, where the lipid transporters are located and signal transductions are initiated. Lysenin is a recently discovered SM-specific cytotoxin (38). Lysenin recognizes SM only when it forms aggregates or microdomains (39). Based on our results above, we anticipated that *Sptlc2* gene deficiency would reduce hepatocyte plasma membrane SM levels and influence the formation of aggregates or microdomains that are recognizable by lysenin. To investigate the effect of liver *Sptlc2* deficiency on the formation of these microdomains, we isolated primary hepatocytes from *Sptlc2* KO and WT mice, and tested the sensitivity of these cells to lysenin-mediated cytolysis. As indicated in Fig. 5A, hepatocytes lacking in *Sptlc2* showed significantly less sensitivity to lysenin-mediated cytolysis than controls. A dose-dependent lysenin effect in WT cells was observed, and this effect was attenuated in *Sptlc2* KO hepatocytes (Fig. 5B). We also added dihydroxyphingosine, a precursor of ceramide and SM, to the cell culture medium and found that there was no significant difference between WT and *Sptlc2* KO hepatocytes when 40 μ M dihydroxyphingosine was used, in terms of their lysenin-mediated

TABLE 3**Liver lipid measurement in liver-specific *Sptlc2* KO and WT mice (LC/MS/MS)**

Values are as follows: mean \pm S.D.; $n = 4-5$. The abbreviations used are as follows: SM, sphingomyelin; PC, phosphatidylcholine; Cer, ceramide; Sph, sphingosine; S-1-P, sphingosine-1-phosphate; DHS-1-P, dihydroxysphingosine-1-phosphate.

Mice	SM	PC	Cer	Sph	S-1-P	DHS-1-P
	$\mu\text{g}/\text{mg liver}$	$\mu\text{g}/\text{mg liver}$	$\text{ng}/\text{mg liver}$	$\text{ng}/\text{mg liver}$	$\text{ng}/\text{mg liver}$	$\text{ng}/\text{mg liver}$
One month						
WT	0.58 ± 0.02	17 ± 1	134 ± 10	2.2 ± 0.3	0.08 ± 0.01	0.12 ± 0.02
<i>Sptlc2</i> KO	0.36 ± 0.01^a	15 ± 2	82 ± 9^a	1.5 ± 0.2^a	0.11 ± 0.02^a	0.13 ± 0.01
Two months						
WT	0.62 ± 0.03	18 ± 2	141 ± 12	1.9 ± 0.2	0.10 ± 0.02	0.15 ± 0.03
<i>Sptlc2</i> KO	0.39 ± 0.04^a	21 ± 4	102 ± 16^a	1.6 ± 0.3	0.13 ± 0.01^a	0.15 ± 0.01

^a Values are $p < 0.05$.

ated cell mortality (Fig. 5C), indicating that supplement of dihydrosphingosine can correct the phenotype caused by *Sptlc2* deficiency. These results suggested that liver *Sptlc2* deficiency not only significantly decreased SM levels in the liver, but also significantly altered the SM-rich microdomains (probably lipid rafts) in the hepatocyte plasma membranes.

Liver *Sptlc2* Deficiency Increases Plasma ApoE Levels—Assessment of plasma apolipoprotein levels by reducing SDS-PAGE revealed a marked increase of apoE, by 3.5-fold ($p < 0.0001$), but no changes in apoB or apoA-I (Fig. 6, A and B). We also measured apoE, apoB, and apoA-I mRNA levels in the liver by real time PCR, finding no significant differences between the AAV-Cre- and AAV-LacZ-treated mice (data not shown). We likewise measured liver apoE, apoB, and apoA-I protein levels (Fig. 6C) and found no changes, indicating that apoE biosynthesis might not be affected.

To examine the effect of SPT deficiency on apoE secretion at a cellular level, we performed metabolic labeling (pulse-chase) experiments on primary hepatocytes derived from *Sptlc2* KO and WT mice. There were marked increases in apoE secretion, 2.5-fold at 1 h and 3.3-fold at 2 h ($n = 4$) ($p < 0.001$) from hepatocytes of AAV-Cre-infected mice, compared with AAV-LacZ-infected ones (Fig. 7B). In contrast, there was no significant difference in apoE accumulation within cells during the chase (Fig. 7A), indicating that control cells might have higher rates of intracellular apoE turnover or that *Sptlc2*-deficient hepatocytes secrete apoE that is more stable than that from control hepatocytes. We also incubated the hepatocytes with different concentration of dihydrosphingosine first and then measured apoE secretion. We found that there was no significant difference between WT and *Sptlc2* KO hepatocytes when 40 μM dihydrosphingosine was used, in terms of apoE secretion (Fig. 7C), indicating that supplement of dihydrosphingosine can correct the phenotype caused by *Sptlc2* deficiency.

Plasma from Liver-specific *Sptlc2*-deficient Mice Promotes Cholesterol Efflux from Macrophages—Macrophage cholesterol efflux plays an important role in reverse cholesterol transport, an anti-atherogenic process. Because apoE levels were increased by 3.5-fold in *Sptlc2* KO mouse plasma, and apoE is a well known factor mediating macrophage cholesterol efflux (40, 41), we speculated that *Sptlc2* KO plasma might promote cholesterol efflux. Thus we investigated the capacity of plasma from liver-specific *Sptlc2*-deficient mice to mediate cholesterol efflux from the mouse macrophage. WT mouse macrophages derived from bone marrow were labeled with [^3H]cholesterol. Cholesterol efflux was monitored after 10% plasma from either

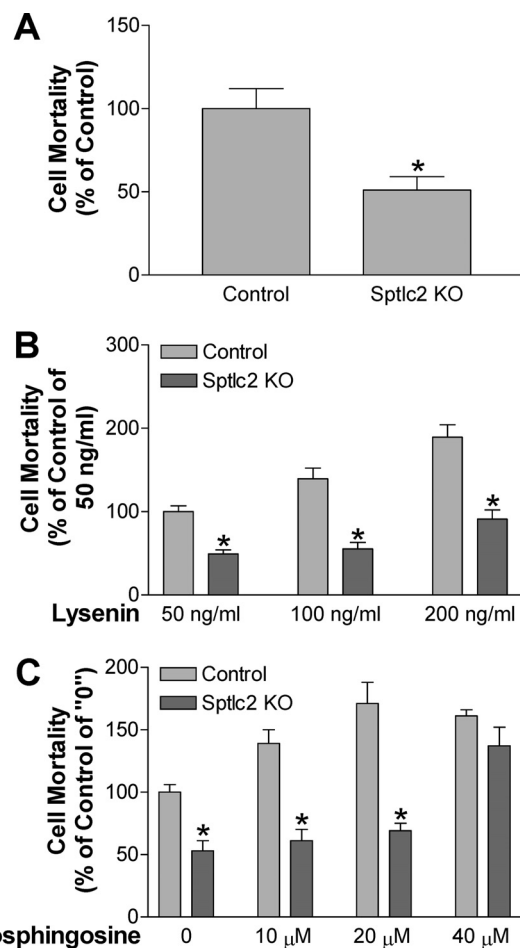


FIGURE 5. Liver-specific *Sptlc2* deficiency decreased lysenin-mediated hepatocyte mortality. Primary hepatocytes were isolated and treated with lysenin. A, cells were treated with lysenin (200 ng/ml) for 2 h. Cell mortality was monitored by WST-1 cell proliferation reagent (Roche Applied Science). B, cells were treated with different concentrations of lysenin for 2 h. C, cells were treated different concentrations of dihydrosphingosine for 4 h and then with lysenin (150 ng/ml) for 2 h. Values are mean \pm S.D., $n = 5$, $p < 0.01$.

WT or *Sptlc2* KO mice was applied to the macrophages. As shown in Fig. 8A, *Sptlc2* KO plasma significantly increased cholesterol efflux from the macrophages, 1.7-fold at 4 h and 2.3-fold at 8 h, compared with plasma from WT mice ($p < 0.01$). To investigate the contribution of apoE, which is enriched in *Sptlc2* KO plasma, we added recombinant apoE to plasma from AAV-LacZ-treated animals prior to assaying for cholesterol efflux, finding that apoE supplementation (4 $\mu\text{g}/\text{ml}$) can significantly increase cholesterol efflux (Fig. 8B). Furthermore, because

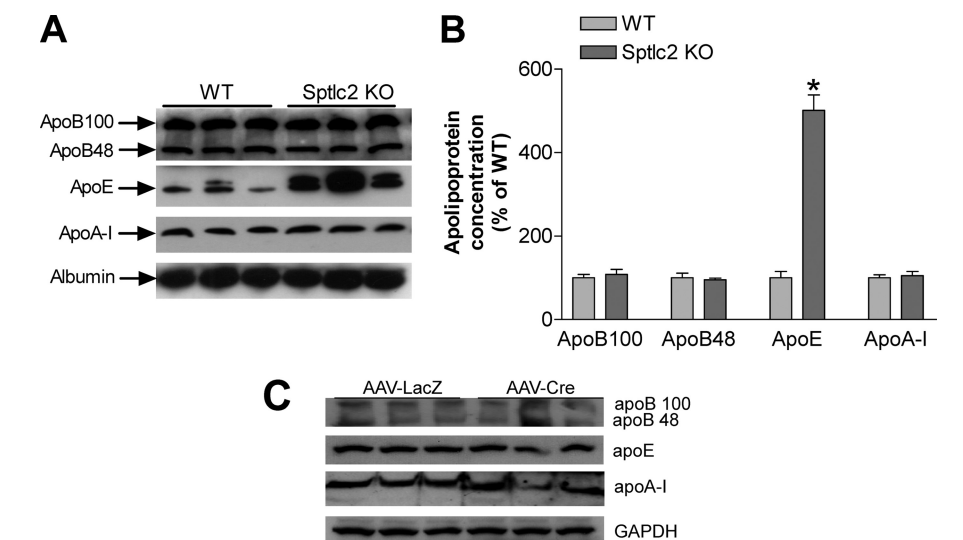


FIGURE 6. Liver-specific *Sptlc2* deficiency significantly increased plasma apoE but not apoB or apoA-I levels. Plasma apoE, apoB, and apoA-I levels were determined as described previously. Briefly, 0.2 μ l plasma was separated by 4–15% SDS-gel electrophoresis and immunoblotted with polyclonal antibodies against apoE (Abcam), apoB (United States Biological), and apoA-I (Abcam). *A*, Western blot of plasma apoA-I, apoB, and apoE, representative of three independent experiments. *B*, quantitative display of plasma apolipoproteins. *C*, Western blot of apoA-I, apoE, and apoE in mouse livers. Values are mean \pm S.D., $n = 5$, $p < 0.001$. *GAPDH*, glyceraldehyde-3-phosphate dehydrogenase.

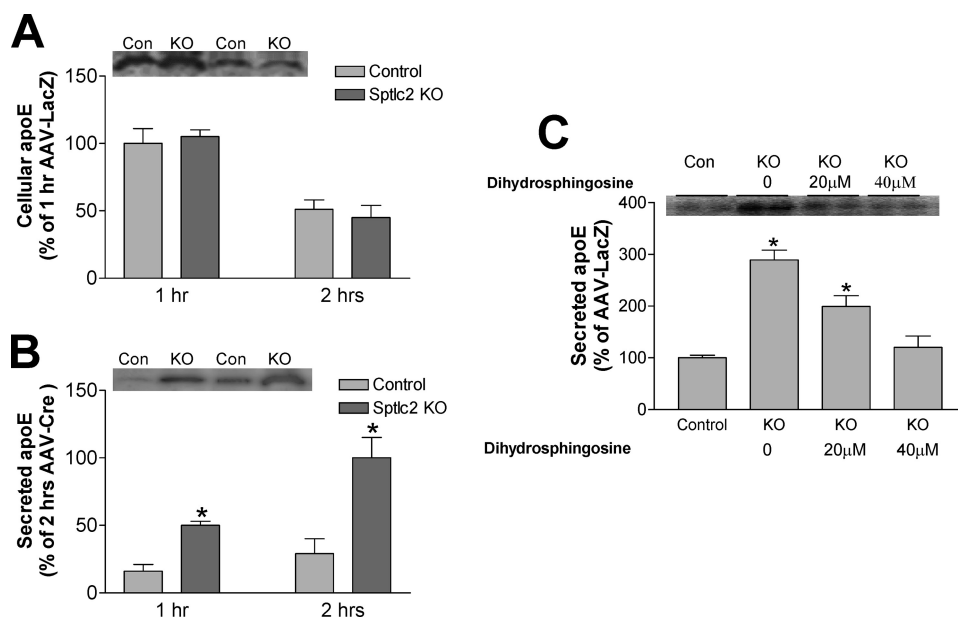


FIGURE 7. *Sptlc2*-deficient hepatocytes secrete more apoE. Primary hepatocytes were labeled with [35 S]methionine, and [35 S]apoE was immunoprecipitated from cell lysate or media as described under "Experimental Procedures." *A*, apoE in cell lysates. *B*, apoE in cell media. *C*, effect of dihydrosphingosine supplementation. Primary hepatocytes were first incubated with 0, 20, and 40 μ M dihydrosphingosine for 4 h and then were used for apoE secretion. Values are mean \pm S.D., $n = 4$, $p < 0.01$. *Con*, control.

liver-specific *Sptlc2*-deficient plasma contains less SM (Table 1), which may also play a role in cholesterol efflux, we supplemented plasma from AAV-Cre-treated animals with SM (20–80 mg/dl) and assayed for cholesterol efflux. We found no significant changes (Fig. 8C), indicating that apoE accumulation, not a decrease in SM, mediates greater cholesterol efflux.

DISCUSSION

In this study, we have demonstrated for the first time that Cre-Lox system disruption of the *Sptlc2* gene in the liver

resulted in the following: 1) loss of SPT activity in the liver, although *Sptlc1* protein levels were not influenced; 2) significant reduction of plasma SM and ceramide levels; 3) significant reduction of liver and hepatocyte plasma membrane SM levels; 4) significant increase of plasma apoE levels in the circulation, but not of apoA-1 and apoB; and 5) significant increase of cholesterol efflux from macrophages into the plasma. Thus, liver-specific SPT deficiency produces an anti-atherogenic phenotype in mice.

SM, a phospholipid located in the surface monolayer of all classes of plasma lipoproteins (1), has significant effects on lipoprotein metabolism. The liver is the major site for lipoprotein production, and this study shows that liver SPT, a key enzyme for SM biosynthesis, contributes roughly 36% to plasma SM levels (Tables 1 and 2).

We found that higher plasma SM levels and SM/PC ratios are independent risk factors for coronary heart disease (19, 20). We believe that LDL retained in atherosclerotic lesions is acted on by an arterial wall sphingomyelinase, which promotes aggregation by converting SM to ceramide (10–12). There are two ways of preventing this atherogenic event, the first being reduction of sphingomyelinase levels. Indeed, it has recently been reported that *apoE* KO mice lacking in sphingomyelinase have decreased development of early atherosclerotic lesions and, more important, decreased retention of atherogenic lipoproteins, compared with *apoE* KO matched for similar plasma lipoprotein levels (14). The second approach for preventing the atherogenic event cited above is through

reduction of SM levels in the atherogenic lipoproteins. This can be done by inhibiting the SM biosynthesis pathway in the lipoprotein-producing tissues, the liver and small intestine. We have found that liver-specific SPT deficiency can significantly decrease SM in the circulation. We observed that a liver SPT deficiency caused a 36% reduction of plasma SM levels (Table 1 and 2). There are three possible explanations for our not observing a larger effect as follows: 1) there may still have been some residual SPT activity after AAV-LacZ treatment (Fig. 2G) in the liver; 2) other organs, for example, the small intestine and lungs, may also make contri-

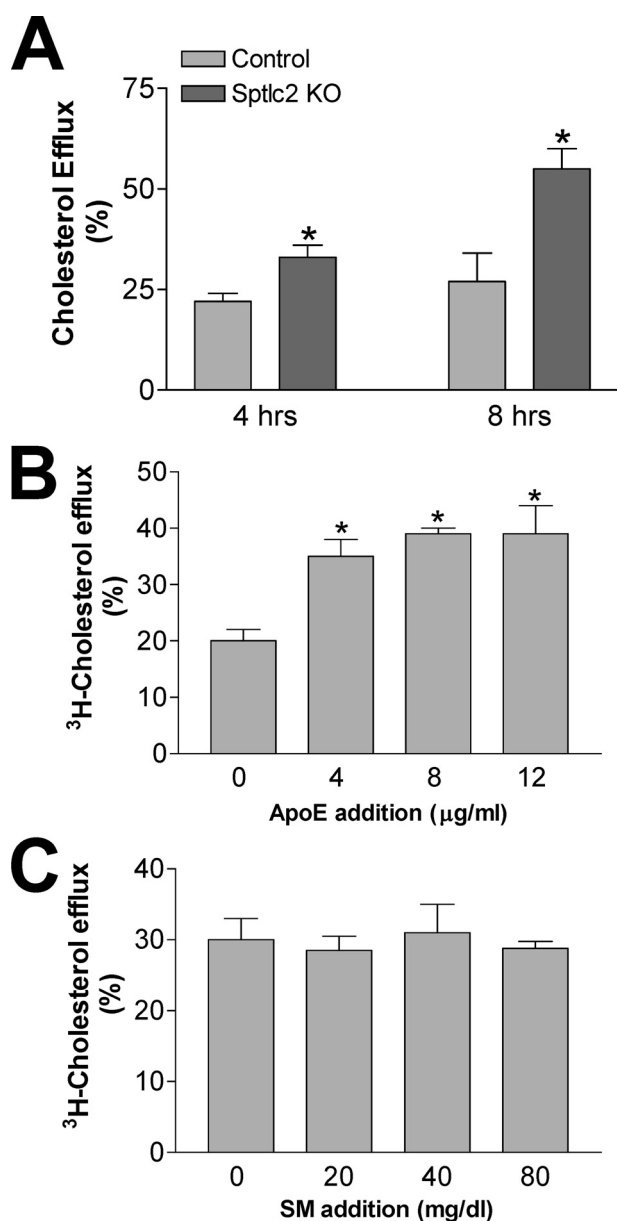


FIGURE 8. Plasma from liver-specific *Sptlc2*-deficient mice promotes cholesterol efflux from macrophages. *A*, wild-type macrophages (10^5 cells/well) were grown in DMEM with 10% FBS. Cell labeling was done by growing the cells overnight in DMEM with 10% FBS containing 50 $\mu\text{g/ml}$ acetylated LDL and 1 $\mu\text{Ci/ml}$ [^3H]cholesterol. Cells were washed with PBS, and the medium was replaced with DMEM containing 10% plasma from WT and liver-specific *Sptlc2* KO mice. [^3H]cholesterol radioactivity in the medium was measured at 4 and 8 h. Radioactivity within the cells was also quantified. The percentage of cholesterol efflux was calculated by dividing the radioactive counts in the extracellular media by the total of radioactive counts in the medium and cell fraction. *B*, plasma from control (AAV-LacZ-treated) mice was supplemented with 4, 8, and 12 $\mu\text{g/ml}$ recombinant apoE, respectively, and cholesterol efflux was performed as above. *C*, plasma from AAV-Cre-treated mice was supplemented with SM (20, 40, and 80 mg/dl, respectively), and cholesterol efflux was performed as above. Values are mean \pm S.D., $n = 4$, $p < 0.01$.

butions to plasma SM levels; and 3) there may be other factors, for example sphingomyelinase, that can influence plasma SM levels.

The lysenin experiment indicated that SPT-deficient liver cells have less SM in the plasma membranes (Fig. 5). Moreover, lysenin only recognizes clusters of SM (38, 39), which exist in microdomains such as lipid rafts. Therefore, an SPT deficiency may influence lipid raft-mediated events such as cholesterol

efflux (42) and cytokine signaling (NF- κ B and tumor necrosis factor- α pathways) (43). The relative proportions of both SM and cholesterol appear critical for raft stability, because depletion of cholesterol or supplementation of the SM pool abolishes or re-establishes, respectively, detergent insolubility of the domains and their sorting capacity (44–47).

In this study, we demonstrated that *Sptlc2* deficiency increases plasma apoE (Fig. 6) and increases apoE secretion from primary hepatocytes (Fig. 7B). It is very likely that SM reduction alters the structure of cellular membranes, thus influencing apoE secretion. However, there is another possibility that changes in ceramide levels may also have an impact on plasma apoE, because ceramide is one of the components of large lipid rafts (48, 49). It has been reported that cellular ceramide levels are inversely related with apoE secretion from macrophages (50). Decreased ceramide in the livers of *Sptlc2* KO mice (Table 3) might be related to increased apoE secretion. Details of this process deserve further investigation.

Liver-specific *Sptlc2* deficiency causes a small but significant increase in plasma cholesterol levels (Table 1). This increase is not related to an increase of liver cholesterol biosynthesis, because hydroxymethylglutaryl-CoA reductase mRNA levels do not change (data not shown). It is known that SM is a cholesterol-binding molecule (51–53). Based on that, we have speculated that SPT deficiency promotes cholesterol efflux through decreasing cellular of cholesterol sequestration by SM. Indeed, it has been reported that sphingomyelinase-deficient macrophages efflux significantly less cholesterol than WT cells, and this is because of sequestration of cholesterol by SM (24). We have also observed that *Sptlc2* heterozygous KO macrophages efflux more cholesterol toward apoA-I and HDL.³

We have confirmed a number of previous observations in this study. For example, we previously reported that homozygous *Sptlc1* or *Sptlc2* conventional KO mice are embryonic lethal (30). In the process of preparing *Sptlc2*-Flox, we found that the Neo-resistant gene must be deleted through breeding to Flp transgenic mice (Fig. 2A) (31, 32). Homozygous *Sptlc2*-Flox mice cannot be obtained if the Neo-resistant gene remains in the middle of intron 1 of the *Sptlc2* gene, impeding RNA processing of the gene. It is known that Sptlc1 and Sptlc2 are subunits of SPT, and both are essential for SPT activity (26–28). This observation was again confirmed here. We found that *Sptlc2* deficiency led to almost complete loss of SPT activity in the liver (Fig. 2G).

In summary, liver-specific SPT deficiency significantly reduced liver and plasma SM levels and significantly increased those of plasma apoE. The atheroprotective impact of this finding is currently being evaluated in our laboratory.

Acknowledgments—We thank Clavin Yeang for the English editing. We also acknowledge the Gene Therapy Resource Program, NHLBI, National Institutes of Health, for providing the gene vectors used in this study.

REFERENCES

1. Nilsson, A., and Duan, R. D. (2006) *J. Lipid Res.* **47**, 154–171
2. Saito, H., Arimoto, I., Tanaka, M., Sasaki, T., Tanimoto, T., Okada, S., and

³ M. Chakraborty and X.-C. Jiang, unpublished observations.

- Handa, T. (2000) *Biochim. Biophys. Acta* **1486**, 312–320
3. Arimoto, I., Saito, H., Kawashima, Y., Miyajima, K., and Handa, T. (1998) *J. Lipid Res.* **39**, 143–151
4. Arimoto, I., Matsumoto, C., Tanaka, M., Okuhira, K., Saito, H., and Handa, T. (1998) *Lipids* **33**, 773–779
5. Rye, K. A., Hime, N. J., and Barter, P. J. (1996) *J. Biol. Chem.* **271**, 4243–4250
6. Subbaiah, P. V., and Liu, M. (1993) *J. Biol. Chem.* **268**, 20156–20163
7. Bolin, D. J., and Jonas, A. (1996) *J. Biol. Chem.* **271**, 19152–19158
8. Subbaiah, P. V., Gesquiere, L. R., and Wang, K. (2005) *J. Lipid Res.* **46**, 2699–2705
9. Williams, K. J., and Tabas, I. (1995) *Arterioscler. Thromb. Vasc. Biol.* **15**, 551–561
10. Hoff, H. F., and Morton, R. E. (1985) *Ann. N.Y. Acad. Sci.* **454**, 183–194
11. Guyton, J. R., and Klemp, K. F. (1996) *Arterioscler. Thromb. Vasc. Biol.* **16**, 4–11
12. Schissel, S. L., Tweedie-Hardman, J., Rapp, J. H., Graham, G., Williams, K. J., and Tabas, I. (1996) *J. Clin. Invest.* **98**, 1455–1464
13. Schissel, S. L., Jiang, X., Tweedie-Hardman, J., Jeong, T., Camejo, E. H., Najib, J., Rapp, J. H., Williams, K. J., and Tabas, I. (1998) *J. Biol. Chem.* **273**, 2738–2746
14. Devlin, C. M., Leventhal, A. R., Kuriakose, G., Schuchman, E. H., Williams, K. J., and Tabas, I. (2008) *Arterioscler. Thromb. Vasc. Biol.* **28**, 1723–1730
15. Rodriguez, J. L., Ghiselli, G. C., Torreggiani, D., and Sirtori, C. R. (1976) *Atherosclerosis* **23**, 73–83
16. Jeong, T. S., Schissel, S. L., Tabas, I., Pownall, H. J., Tall, A. R., and Jiang, X. (1998) *J. Clin. Invest.* **101**, 905–912
17. Zhang, S. H., Reddick, R. L., Piedrahita, J. A., and Maeda, N. (1992) *Science* **258**, 468–471
18. Plump, A. S., and Breslow, J. L. (1995) *Annu. Rev. Nutr.* **15**, 495–518
19. Jiang, X. C., Paultre, F., Pearson, T. A., Reed, R. G., Francis, C. K., Lin, M., Berglund, L., and Tall, A. R. (2000) *Arterioscler. Thromb. Vasc. Biol.* **20**, 2614–2618
20. Schlitt, A., Blankenberg, S., Yan, D., von Gizycki, H., Buerke, M., Werdan, K., Bickel, C., Lackner, K. J., Meyer, J., Rupprecht, H. J., and Jiang, X. C. (2006) *Nutr. Metab.* **3**, 5
21. Simons, K., and Ikonen, E. (1997) *Nature* **387**, 569–572
22. Simons, K., and Ikonen, E. (2000) *Science* **290**, 1721–1726
23. Li, Z., Hailemariam, T. K., Zhou, H., Li, Y., Duckworth, D. C., Peake, D. A., Zhang, Y., Kuo, M. S., Cao, G., and Jiang, X. C. (2007) *Biochim. Biophys. Acta* **1771**, 1186–1194
24. Leventhal, A. R., Chen, W., Tall, A. R., and Tabas, I. (2001) *J. Biol. Chem.* **276**, 44976–44983
25. Merrill, A. H., Jr., and Jones, D. D. (1990) *Biochim. Biophys. Acta* **1044**, 1–12
26. Weiss, B., and Stoffel, W. (1997) *Eur. J. Biochem.* **249**, 239–247
27. Hanada, K., Hara, T., Nishijima, M., Kuge, O., Dickson, R. C., and Nagiec, M. M. (1997) *J. Biol. Chem.* **272**, 32108–32114
28. Yasuda, S., Nishijima, M., and Hanada, K. (2003) *J. Biol. Chem.* **278**, 4176–4183
29. Hornemann, T., Richard, S., Rütli, M. F., Wei, Y., and von Eckardstein, A. (2006) *J. Biol. Chem.* **281**, 37275–37281
30. Hojjati, M. R., Li, Z., and Jiang, X. C. (2005) *Biochim. Biophys. Acta* **1737**, 44–51
31. Farley, F. W., Soriano, P., Steffen, L. S., and Dymecki, S. M. (2000) *Genesis* **28**, 106–110
32. Jones, J. R., Shelton, K. D., and Magnuson, M. A. (2005) *Methods Mol. Med.* **103**, 245–257
33. Kitajima, K., Marchadier, D. H., Miller, G. C., Gao, G. P., Wilson, J. M., and Rader, D. J. (2006) *Arterioscler. Thromb. Vasc. Biol.* **26**, 1852–1857
34. Hojjati, M. R., and Jiang, X. C. (2006) *J. Lipid Res.* **47**, 673–676
35. Rohlmann, A., Gotthardt, M., Hammer, R. E., and Herz, J. (1998) *J. Clin. Invest.* **101**, 689–695
36. Liebisch, G., Lieser, B., Rathenberg, J., Drobnik, W., and Schmitz, G. (2004) *Biochim. Biophys. Acta* **1686**, 108–117
37. Jiang, X. C., Li, Z., Liu, R., Yang, X. P., Pan, M., Lagrost, L., Fisher, E. A., and Williams, K. J. (2005) *J. Biol. Chem.* **280**, 18336–18340
38. Yamaji, A., Sekizawa, Y., Emoto, K., Sakuraba, H., Inoue, K., Kobayashi, H., and Umeda, M. (1998) *J. Biol. Chem.* **273**, 5300–5306
39. Ishitsuka, R., Yamaji-Hasegawa, A., Makino, A., Hirabayashi, Y., and Kobayashi, T. (2004) *Biophys. J.* **86**, 296–307
40. Innerarity, T. L., Pitas, R. E., and Mahley, R. W. (1982) *Arteriosclerosis* **2**, 114–124
41. Gordon, V., Innerarity, T. L., and Mahley, R. W. (1983) *J. Biol. Chem.* **258**, 6202–6212
42. Landry, Y. D., Denis, M., Nandi, S., Bell, S., Vaughan, A. M., and Zha, X. (2006) *J. Biol. Chem.* **281**, 36091–36101
43. Hailemariam, T. K., Huan, C., Liu, J., Li, Z., Roman, C., Kalbfeisch, M., Bui, H. H., Peake, D. A., Kuo, M. S., Cao, G., Wadgaonkar, R., and Jiang, X. C. (2008) *Arterioscler. Thromb. Vasc. Biol.* **28**, 1519–1526
44. Brown, D. A., and London, E. (2000) *J. Biol. Chem.* **275**, 17221–17224
45. Keller, P., and Simons, K. (1998) *J. Cell Biol.* **140**, 1357–1367
46. Hoekstra, D., and van IJzendoorn, S. C. (2000) *Curr. Opin. Cell Biol.* **12**, 496–502
47. Gkantiragas, I., Brügger, B., Stüven, E., Kaloyanova, D., Li, X. Y., Löhr, K., Lottspeich, F., Wieland, F. T., and Helms, J. B. (2001) *Mol. Biol. Cell* **12**, 1819–1833
48. Grassme, H., Jekle, A., Riehle, A., Schwarz, H., Berger, J., Sandhoff, K., Kolesnick, R., and Gulbins, E. (2001) *J. Biol. Chem.* **276**, 20589–20596
49. Grassmé, H., Jendrosseck, V., Bock, J., Riehle, A., and Gulbins, E. (2002) *J. Immunol.* **168**, 298–307
50. Lucic, D., Huang, Z. H., Gu, D., Subbaiah, P. V., and Mazzone, T. (2007) *Biochemistry* **46**, 11196–11204
51. Grönberg, L., Ruan, Z. S., Bittman, R., and Slotte, J. P. (1991) *Biochemistry* **30**, 10746–10754
52. McIntosh, T. J., Simon, S. A., Needham, D., and Huang, C. H. (1992) *Biochemistry* **31**, 2020–2024
53. Ridgway, N. D. (2000) *Biochim. Biophys. Acta* **1484**, 129–141